THE JOURNAL OF PHYSICAL CHEMISTRY B

Article

pubs.acs.org/JPCB

Intermolecular/Interionic Vibrations of 1-Methyl-3-*n*-octylimidazolium Tetrafluoroborate Ionic Liquid and H_2O Mixtures

Hideaki Shirota*,† and Ranjit Biswas*,‡

†Department of Nanomaterial Science & Department of Chemistry, Chiba University, 1-33 Yayoi, Inage-ku, Chiba 263-8522, Japan

‡Chemical, Biological and Macromolecular Sciences, S. N. Bose National Centre for Basic Sciences, J. D. Block, Sec.III, Salt Lake, Kolkata 700 098, West Bengal, India

ABSTRACT: We report here the low-frequency spectra, resulting from the intermolecular/interionic vibrational dynamics, of aqueous mixtures of an ionic liquid, 1-methyl-3-*n*-octylimidazolium tetrafluoroborate, with the H_2O mole fractions of 0.2, 0.4, and 0.6 and the neat ionic liquid and H_2O within the frequency range of 0.1−700 cm^{-1} by means of femtosecond Raman-induced Kerr effect spectroscopy. Addition of H_2O induces tiny effects on the line shape of the low-frequency Kerr spectrum of the ionic liquid: ca. a 2 cm^{-1} red shift in the first moment of the low-frequency spectrum has been observed for a transition from the neat ionic liquid to the binary mixture containing 0.6 mol fraction of H_2O. Surface tension and liquid density of the mixture also accompany minimal changes upon addition of H_2O. These results suggest that H_2O molecules localize at the interface between the ionic and nonpolar regions, and the interionic interaction in the ionic region is weakly perturbed by the existence of H_2O. On the other hand, successive addition of H_2O in the mixture slows down the picosecond overdamped relaxation process measured in the 3−300 ps range even though the shear viscosity of the mixture decreases substantially.

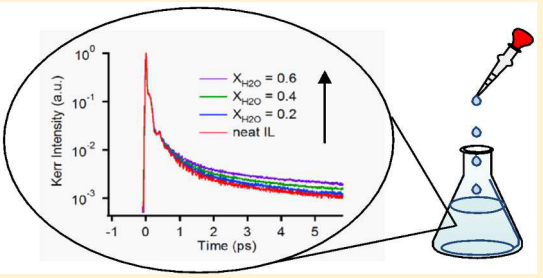

1. INTRODUCTION

One of the unique natures of ionic liquid (IL) is its microheterogeneous structure.[1−18] The microheterogeneous structure in IL is a result of microscopic phase segregation because of the presence of two different polarity parts: a nonpolar group and ions or ionic moieties. The microscopic phase segregation is therefore more pronounced in an IL whose ion possesses a longer alkyl group. Indeed, a great dissolving power of IL for a wide variety of solutes, e.g., organic/inorganic compounds, salts, and polymers, can actually be attributed to this microheterogeneous liquid structure. Accordingly, it is important to study mixtures of IL along with neat ILs, not only for understanding the fundamental scientific aspects of IL but also for exploring the suitability as alternative reaction media.[19,20]

Mixtures of IL with H_2O and other organic solvents have now been studied more extensively. The solution structure of IL mixtures at the molecular level is much more complicated than conventional solvent mixtures because of the microheterogeneous structure of neat IL itself. Vibrational spectroscopic techniques are very useful in accessing information on the microscopic structure, interaction, and dynamics of condensed phases and thus suitable for studying binary mixtures of ILs with H_2O and other solvents. Although a majority of reported vibrational spectroscopic studies of IL mixtures involve decoding of intramolecular/intraionic vibrational modes including librational and interaction-induced motions by means of traditional FT-IR, far-IR, and Raman spectroscopic measurements,[21−31] a limited number of more sophisticated measurements via femtosecond Raman-induced Kerr effect spectroscopy (fs-RIKES),[32−34] terahertz time domain spectroscopy (THz-TDS),[35] and time-resolved IR spectroscopy[36] are also available. The first two time-resolved measurements mentioned above can detect the low-frequency intermolecular/interionic vibrations in condensed phases. The intermolecular/interionic vibrational band, located in the low-frequency region below 150 cm^{-1}, is directly influenced by the microscopic intermolecular interactions and structure in a given medium, and thus it can efficiently probe the molecular-level aspects of a given sample. Since an understanding of the microscopic interaction, structure, and dynamics is an important prerequisite for developing a molecular level knowledge of solutions and neat liquids, applications of time-resolved vibrational spectroscopies are crucial for ILs, particularly because of the microheterogeneity in neat IL and possible modifications of it upon addition of another solvent into it. The presence of charge−charge interactions renders the situation even more complicated because charge fluctuations in these media are supposed to involve longer length scales than in common organic solvents, but a large inverse Debye screening length is also expected to shorten this interaction length scale.[37] Consequently, the intermolecular/interionic

Received: July 27, 2012
Revised: October 23, 2012

dx.doi.org/10.1021/jp307436t | *J. Phys. Chem. B* XXXX, XXX, XXX−XXX

dynamics in ILs and IL mixtures probed by these time-resolved vibrational spectroscopic techniques carry relatively more microscopic information, and thus the corresponding results can be interpreted in terms of the molecular-level aspects of the structure and dynamics of these media.

Using the THz-TDS technique, Bonn and co-workers first carried out dielectric measurements in the terahertz region of 0.1−1.2 THz (corresponds to ca. 5−40 cm^{-1}) for aqueous mixtures of 1-butyl-3-methylimidazolium tetrafluoroborate ([BMIm][BF_4]−H_2O).[35] Since the THz-TDS technique is responsive to the time-dependent fluctuation in the collective dipole moment−dipole moment correlation function and since the motions of H_2O molecules in the THz region are more IR active than those of the IL, the interaction and dynamics of H_2O in the IL−H_2O mixtures are dominantly observed in this spectroscopic technique. In addition, these results have revealed a nonlinear mixture composition dependence of the relaxation times, the most pronounced effect being in the IL concentration regime between 40 and 90 vol %. Recent combined fs-RIKES and molecular dynamics (MD) simulation studies have revealed in detail the microscopic aspects of mixtures of 1-methyl-3-pentylimidazolium bis-(trifluoromethylsulfonyl)amide with carbon disulfide (CS_2)[33] and acetonitrile.[34] It has been shown that the nonpolar solvent, CS_2, is localized in the nonpolar region of the IL in the low solvent mole fraction region ($X < 0.1$), but the polar solvent, acetonitrile, locates at the interfacial region between the ionic and nonpolar regions. These results indicate that the microscopic structure in IL mixtures sensitizes the location of the added solvent molecules.

In this study, we have investigated the low-frequency intermolecular/interionic vibrational dynamics of mixtures of an IL, 1-methyl-3-*n*-octylimidazolium tetrafluoroborate ([MOIm][BF_4], Scheme 1), with H_2O by means of fs-RIKES, for the first time. This choice of the sample system is motivated by the fact that this aqueous mixture is expected to show a pronounced heterogeneity effect as the [MOIm][BF_4]−H_2O mixture undergoes a phase separation at approximately 0.7 mol fraction of H_2O ($X \approx 0.7$).[30,38,39] As briefly mentioned already, fs-RIKES is a powerful spectroscopic technique to study the low-frequency intermolecular dynamics in condensed phases. This spectroscopic technique has been used to investigate simple molecular liquids,[40−45] but the horizon is now expanding to various complex condensed phases[46−48] including ILs.[18,49,50] In contrast to THz-TDS, fs-RIKES detects the time-dependent fluctuation in the anisotropic part of the collective polarizability tensor−polarizability tensor correlation function (the traditional RIKES polarization condition detects the anisotropic response,[40−45] but it is also possible to probe the isotropic response by controlling the polarization condition[51−53]). Accordingly, it is expected that fs-RIKES dominantly captures the collective dynamics of IL, not of H_2O, since the aromatic cation based IL is more polarizable than H_2O (Raman activity). The present study thus focuses mainly on the intermolecular/interionic motions of IL in IL−H_2O mixtures, which is complementary to the THz-TDS study by Bonn and co-workers.[35]

Scheme 1

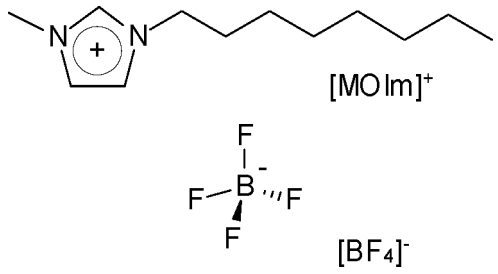

2. EXPERIMENTAL SECTION

[MOIm][BF_4] (Iolitec, 99%) was used, after it was dried in vacuo (ca. 10^{-3} Torr) at 313 K for over 36 h. The H_2O content of the [MOIm][BF_4] was estimated to be 32.2 ppm by Karl Fischer titration using a coulometer (Hiranuma, AQ-300). H_2O (Wako Pure Chemical, ultratrace analysis grade) for the sample mixtures was used as received.

Shear viscosities (η) of the [MOIm][BF_4]−H_2O mixtures, neat [MOIm][BF_4], and neat H_2O were measured by a reciprocating electromagnetic piston viscometer (Cambridge Viscosity, ViscoLab 4100) equipped with a circulating water bath (Yamato, BB300) at 293.0 ± 0.2 K. Surface tensions (γ) of the samples were measured by using a duNouy tensiometer (Yoshida Seisakusho) at 293.0 ± 0.3 K. Densities (d) of the samples were obtained using a volumetric flask at 293.0 ± 0.3 K.

Details of the femtosecond optical heterodyne-detected RIKES setup used here were already reported elsewhere.[45,54] The light source for the most current RIKES setup was a titanium sapphire laser (KMLabs Inc., Griffin) pumped by a Nd:VO_4 diode laser (Spectra Physics, Millennia Pro 5sJ).[55] The output power of the titanium sapphire laser was approximately 420 mW. The typical temporal response, which was the cross-correlation between the pump and probe pulses measured using a 200 μm thick KDP crystal (type I), was 35 ± 3 fs (full width at half-maximum). The scans with high time resolution of 2048 points at 0.5 μm/step were performed for a short time window (6.8 ps). Long time window transients (~300 ps: the maximum time window limited due to the length of the delay stage in the present RIKES setup) were recorded with a data acquisition of 30.0 μm/step. Pure heterodyne signals were achieved by combining the transients recorded at ~1.5° rotations of the input polarizer on both positive and negative orientations to eliminate the residual homodyne signal. For the samples of [MOIm][BF_4]−H_2O mixtures and neat [MOIm]-[BF_4], three scans and six scans for each polarization measurement were averaged, respectively, for the short-time window transients and the long-time window transients. In the case of pure H_2O, however, six scans for each polarization measurement were averaged (short-time window transient only) because of the weak signal compared to the IL mixtures. Prior to the femtosecond RIKES measurements, the samples were injected into a 3 mm optical-path-length quartz cell (Tosoh Quartz) using either a 0.2 or 0.02 μm Anotop filter (Whatman). All the RIKES measurements were made at 293 ± 1 K.

3. RESULTS

Table 1 summarizes the values measured for d, η, and γ of the [MOIm][BF_4]−H_2O mixtures, neat [MOIm][BF_4], and H_2O at 293 K. The data for neat [MOIm][BF_4] and H_2O estimated in this study are in good agreement with the reported values.[56−59] As seen in Table 1, d and γ in the [MOIm]-[BF_4]−H_2O mixtures vary little with the H_2O molar fraction X

dx.doi.org/10.1021/jp307436t | J. Phys. Chem. B XXXX, XXX, XXX−XXX

Table 1. Density d, Shear Viscosity η, and Surface Tension γ of [MOIm][BF_4]−H_2O Mixtures and Neat [MOIm][BF_4] and H_2O at 293 K

X	$d^{a,b}$ (g/dm^3)	$\eta^{c,d}$ (cP)	$\gamma^{e,f}$ (mN/m)
0.0 (IL)	1.102	437	33.9
0.2	1.101	189	34.0
0.4	1.097	87.7	34.1
0.6	1.088	41.8	34.2
1.0 (H_2O)	1.002	0.984	70.8

[a]293.0 ± 0.3 K. [b]±1%. [c]293.0 ± 0.2 K. [d]±5%. [e]293.0 ± 0.3 K. [f]±5%.

and thus exhibit a very weak dependence on X. Although we cannot find any earlier report on d and γ of [MOIm][BF_4]−H_2O mixtures, a similar feature has already been observed in aqueous mixtures of other imidazolium cation based ILs with $[BF_4]^-$ as anion, such as 1-hexyl-3-methylimidazolium tetrafluoroborate and [BMIm][BF_4].[60−62] Following are the probable reasons for the observed weak X dependence of γ: (i) the volume fraction of the nonpolar moiety in [MOIm]-[BF_4]−H_2O mixtures within the X range of 0−0.6 is larger, and this component dominantly contributes to γ, and (ii) as in the cases for aqueous amphiphilic surfactant solutions, H_2O is unlikely to locate itself at the solution surface; the amphiphilic cation probably covers the surface of the solutions. In contrast, η depends strongly on X; the larger the X in the mixture, the lower is η. For example, η of neat [MOIm][BF_4] decreases by approximately an order of magnitude upon addition of 0.6 of X in [MOIm][BF_4], as shown in Table 1. This trend is in qualitative agreement with the results of Sturlaugson et al., although the values of η measured here are somewhat larger than those in their report.[38]

Figure 1 shows (a) the short time window Kerr transients and (b) the long time window Kerr transients of the [MOIm][BF_4]−H_2O mixtures. The Kerr transient of neat H_2O is also shown in Figure 1(a). They are normalized in the intensity at $t = 0$. It is clear from Figure 1(b) that the early part of the overdamped relaxation process in the [MOIm][BF_4]−H_2O mixtures slows down upon increasing X but with a concomitant increase in the decay rate at the later stage. For example, the Kerr transient of neat [MOIm][BF_4] appears to reach a plateau after 200 ps, but that of the [MOIm][BF_4]−H_2O mixture with $X = 0.6$ is decaying even beyond 300 ps. We will elaborate on this feature in the Discussion section. Except for neat H_2O, the following triexponential function with an offset parameter has been used to fit the long time decay of the Kerr transients in the time range 3−300 ps: $a_0 + \Sigma_{i=1}^{3} a_i \exp(-t/\tau_i)$. The fit curves are also shown in Figure 1(b). The Kerr transient decay of neat H_2O within the time range 3−5.8 ps has been analyzed by an exponential function. The fit parameters for the overdamped relaxation process of the [MOIm][BF_4]−H_2O mixtures and neat H_2O are summarized in Table 2. The values of the average time, $\langle\tau\rangle = \Sigma_{i=1}^{3} a_i\tau_i/\Sigma_{i=1}^{3} a_i$, are also listed in Table 2.

The short time window Kerr transients are analyzed by the Fourier-transform deconvolution method by McMorrow and Lotshaw.[63,64] Figure 2 displays the Fourier transform Kerr spectra within the frequency range 0−700 cm^{-1} of (a) the [MOIm][BF_4]−H_2O mixture with $X = 0.4$ and (b) neat H_2O. Here, the picosecond overdamped relaxation process denotes the Kerr transient expressed by a triexponential function with an offset parameter. Note, however, that the fast exponential component ($a_1 \exp(-t/\tau_1)$) is not included in this relaxation

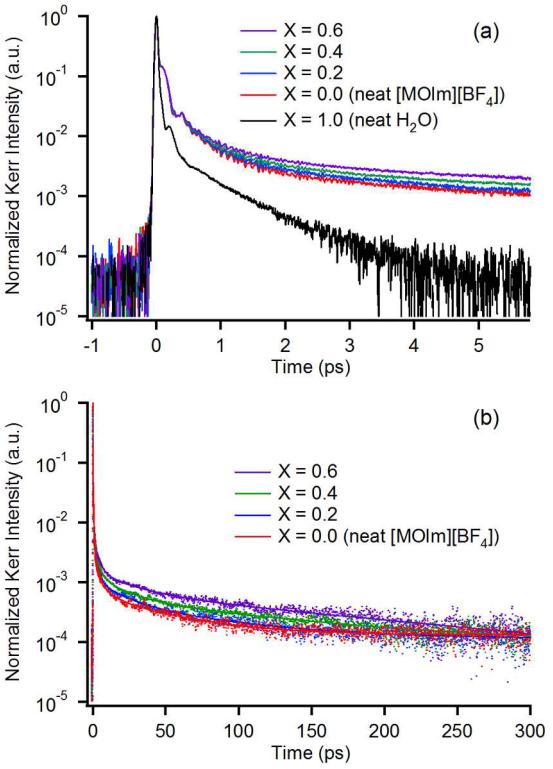

Figure 1. (a) Short time window Kerr transients of [MOIm][BF_4]−H_2O mixtures and neat [MOIm][BF_4] and H_2O. (b) Long time window Kerr transients and their triexponential fits from 3 ps for neat [OMIm][BF_4] and [MOIm][BF_4]−H_2O mixtures.

process because this component has the similar time scale of the intermolecular vibrations or related relaxation process in condensed phases.[45,65−67] As shown in Figure 2, the strong intensity at a frequency near zero (0 cm^{-1}), but not exactly 0 cm^{-1}, in the [MOIm][BF_4]−H_2O mixture is due to the picosecond overdamped relaxation process.

Since the present study focuses on the contribution of the interionic/intermolecular vibrations, we discuss here the spectra obtained after subtracting the contributions of the picosecond overdamped relaxation processes from all the dynamics observed by fs-RIKES. The results are shown in Figure 3. While Figure 3(a) compares the Kerr spectra at various X in the [MOIm][BF_4]−H_2O mixture within the frequency range of 0−700 cm^{-1}, Figure 3(b) highlights the low-frequency region (<250 cm^{-1}) for a more careful examination. It is found from the Fourier transform Kerr spectra that (i) the line shape of the Kerr spectrum of the [MOIm][BF_4]−H_2O mixture is very different from that for neat H_2O and that (ii) the low-frequency Kerr spectrum of the [MOIm][BF_4]−H_2O mixture is rather insensitive to X, showing only a tiny low-frequency shift upon addition of H_2O in [MOIm][BF_4] (for example, a red shift of ∼2 cm^{-1} for increasing X from 0 to 0.6, shown in Table 3, vide infra).

The lineshapes of the low-frequency Kerr spectra within the frequency range 0−250 cm^{-1} are further analyzed. On the basis of our previous works on ILs,[68−75] a sum of Ohmic function, which is the simplest form of the Bucaro−Litovitz function,[76] and antisymmetrized Gaussian functions is used as a line shape model function. This line shape model was originally introduced to fit the low-frequency Kerr spectrum in molecular liquids by Chang and Castner.[77] This has also been used for the

dx.doi.org/10.1021/jp307436t | J. Phys. Chem. B XXXX, XXX, XXX−XXX

Table 2. Triexponential Fit Parameters for Kerr Transients in [MOIm][BF_4]–H_2O Mixtures

X	a_0	a_1 ($a_1/(a_1 + a_2 + a_3)$)	τ_1 (ps)	a_2 ($a_2/(a_1 + a_2 + a_3)$)	τ_2 (ps)	a_3 ($a_3/(a_1 + a_2 + a_3)$)	τ_3 (ps)	$\langle\tau\rangle$ (ps)
0.0 (IL)	0.000132 ± 0.000002	0.002748 ± 0.000102 (0.713)	2.20 ± 0.22	0.000612 ± 0.000181 (0.159)	7.84 ± 1.90	0.000495 ± 0.000034 (0.128)	46.17 ± 2.53	8.72
0.2	0.000114 ± 0.000004	0.003649 ± 0.000070 (0.783)	2.30 ± 0.08	0.000596 ± 0.000042 (0.128)	16.74 ± 2.38	0.000414 ± 0.000054 (0.089)	69.97 ± 7.55	10.17
0.4	0.000089 ± 0.000009	0.003350 ± 0.000038 (0.716)	2.65 ± 0.07	0.000833 ± 0.000032 (0.178)	16.99 ± 1.24	0.000494 ± 0.000020 (0.106)	114.63 ± 9.30	17.07
0.6	0.000005 ± 0.000004	0.003707 ± 0.000039 (0.706)	3.21 ± 0.08	0.000855 ± 0.000039 (0.163)	24.48 ± 2.54	0.000686 ± 0.000020 (0.131)	182.77 ± 34.75	30.20
1.0 (H_2O)	0	0.001238 ± 0.000153	1.44 ± 0.07					

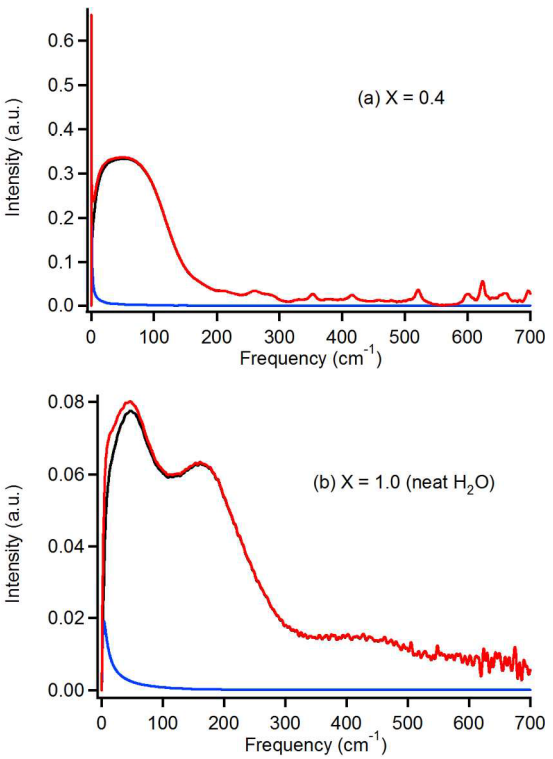

Figure 2. Fourier transform Kerr spectra with the frequency range of 0–700 cm^{-1} of (a) [MOIm][BF_4]–H_2O with X = 0.4 and (b) neat H_2O. Red lines denote the entire Kerr spectra; blue lines denote the contribution of the overdamped relaxation process; and black lines denote the Kerr spectra subtracted the component of the overdamped relaxation process.

low-frequency Kerr spectra of neat ILs and IL mixtures/solutions not only by us[68−75] but also by Quitevis and co-workers though they used the Bucaro–Litovitz function instead of the Ohmic function.[10,32−34,78−83] Ohmic function is defined as

$$I_O(\omega) = a_O \omega \exp(-\omega/\omega_O) \quad (1)$$

where a_O and ω_O are the amplitude and characteristic frequency parameters of the Ohmic line shape, respectively. The antisymmetrized Gaussian function is given by

$$I_{G,i}(\omega) = \sum_{i=1}^{3} a_{G,i} \exp\left[\frac{-2(\omega - \omega_{G,i})^2}{\Delta\omega_{G,i}^2}\right] - a_{G,i} \exp\left[\frac{-2(\omega + \omega_{G,i})^2}{\Delta\omega_{G,i}^2}\right] \quad (2)$$

where $a_{G,i}$, $\omega_{G,i}$, and $\Delta\omega_{G,i}$ are the amplitude, characteristic frequency, and bandwidth parameters for the i-th antisymmetrized Gaussian function, respectively. Since the spectra of [MOIm][BF_4]–H_2O mixtures include shoulder/structure at ca. 170 and 210 cm^{-1} and some imidazolium ILs with relatively small anions which are composed of a small number of atoms (for example, 1-butyl-3-methylimidazolium thiocyanate[74] and 1-butyl-3-methylimidazolium hexafluorophosphate[71]) show intraionic vibrational modes at these frequency regions, a Lorentzian function is used to fit each frequency region. A Lorentzian function is

dx.doi.org/10.1021/jp307436t | J. Phys. Chem. B XXXX, XXX, XXX–XXX

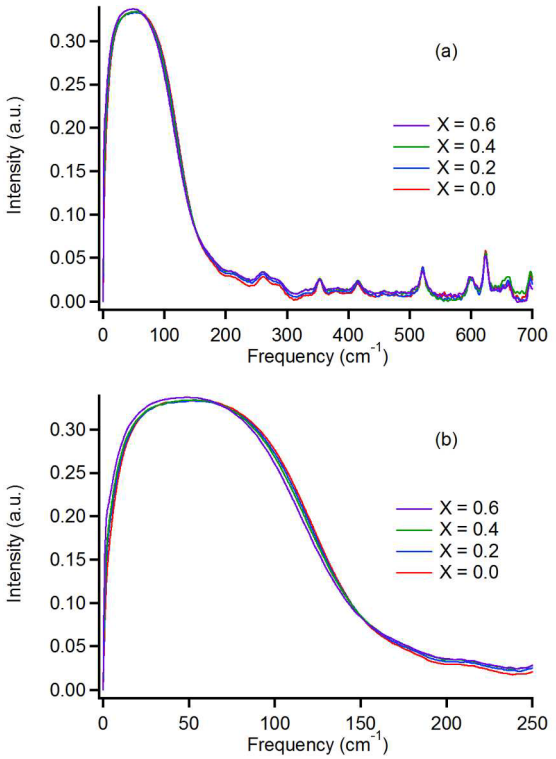

Figure 3. Fourier transform Kerr spectra subtracted the component of the overdamped relaxation process with the frequency range of 0−700 cm^{-1} of (a) neat [OMIm][BF_4] and [MOIm][BF_4]−H_2O mixtures. (b) Highlight of Fourier transform Kerr spectra with the frequency range of 0−250 cm^{-1}.

$$I_L(\omega) = \frac{a_L}{(\omega - \omega_L)^2 + \Delta\omega_L{}^2} \quad (3)$$

where a_L, ω_L, and $\Delta\omega_L$ are the amplitude, peak frequency, and bandwidth parameters, respectively. To fit the low-frequency spectra within the frequency range 0−240 cm^{-1} for the [MOIm][BF_4]−H_2O mixtures, one Ohmic function, three antisymmetrized Gaussian functions, and two Lorentzian functions are used. Figure 4 shows the low-frequency Kerr spectra of (a) neat [MOIm][BF_4] (X = 0.0), (b) a [MOIm][BF_4]−H_2O mixture with X = 0.4, and (c) neat H_2O (X = 1.0) and their fits. Note that the displayed frequency scale for neat [MOIm][BF_4] and the [MOIm][BF_4]−H_2O mixture (X = 0.4) is 250 cm^{-1}, and the fit range is from 0 to 240 cm^{-1}; however, the frequency scale for neat H_2O is 700 cm^{-1}, and the fit range is from 0 to 700 cm^{-1}. Fits of similar quality have also been obtained for the low-frequency Kerr spectra of other samples as well. The fit parameters are summarized in Table 3. The intraionic vibrational bands at ca. 172 and 214 cm^{-1} are attributed to the torsional modes of the octyl group of the [MOIm]$^+$ cation since 1-butyl-3-methylimidazolium cation based ILs with simple anions show intraionic vibrational bands at similar frequencies, which are attributed to the cation.[71,74] The first moment M_1 of the spectrum is estimated by

$$M_1 = \int \omega I(\omega) d\omega / \int I(\omega) d\omega \quad (4)$$

where $I(\omega)$ is the frequency-dependent spectral intensity estimated from the fit analysis (sum of eqs 1 and 2). The integral frequency range is from 0 to 1000 cm^{-1}. Note that we

Table 3. Fit Parameters for Fourier Transform Kerr Spectra of [MOIm][BF_4]−H_2O Mixtures[a]

X	M_1[b] (cm^{-1})	a_O	ω_O (cm^{-1})	$a_{G,1}$	$\omega_{G,1}$ (cm^{-1})	$\Delta\omega_{G,1}$ (cm^{-1})	$a_{G,2}$	$\omega_{G,2}$ (cm^{-1})	$\Delta\omega_{G,2}$ (cm^{-1})	$a_{G,3}$	$\omega_{G,3}$ (cm^{-1})	$\Delta\omega_{G,3}$ (cm^{-1})
0.0 (IL)	70.26	0.063 ± 0.001	3.38 ± 0.02	0.148 ± 0.057	7.20 ± 3.01	24.42 ± 1.46	0.307 ± 0.263	15.80 ± 14.50	57.45 ± 6.43	0.294 ± 0.003	83.44 ± 0.57	79.02 ± 0.54
0.2	69.78	0.091 ± 0.001	2.82 ± 0.01	0.146 ± 0.044	6.97 ± 2.25	22.40 ± 1.18	0.238 ± 0.071	17.19 ± 5.59	51.84 ± 3.10	0.302 ± 0.001	79.25 ± 0.36	82.74 ± 0.38
0.4	69.45	0.109 ± 0.001	2.53 ± 0.01	0.158 ± 0.069	6.08 ± 2.87	21.07 ± 1.35	0.197 ± 0.034	17.48 ± 3.31	47.12 ± 2.03	0.310 ± 0.001	74.70 ± 0.25	87.02 ± 0.29
0.6	68.42	0.182 ± 0.001	1.93 ± 0.01	0.176 ± 0.096	4.92 ± 2.91	18.00 ± 1.25	0.203 ± 0.045	14.36 ± 3.60	42.74 ± 1.89	0.321 ± 0.001	68.47 ± 0.23	92.22 ± 0.29
1.0 (H_2O)	225.97	0.009 ± 0.001	9.73 ± 0.05	0.068 ± 0.001	36.09 ± 0.92	77.24 ± 0.84	0.053 ± 0.001	156.71 ± 0.19	129.77 ± 0.33	0.015 ± 0.001	334.18 ± 4.06	528.69 ± 5.17
X		$a_{L,1}$		$\omega_{L,1}$ (cm^{-1})		$\Delta\omega_{L,1}$ (cm^{-1})		$a_{L,2}$		$\omega_{L,2}$ (cm^{-1})		$\Delta\omega_{L,2}$ (cm^{-1})
0.0 (IL)		8.040 ± 0.556		173.11 ± 0.15		21.05 ± 0.49		28.043 ± 0.992		214.02 ± 0.30		35.39 ± 0.51
0.2		7.349 ± 0.626		173.10 ± 0.19		21.13 ± 0.59		45.452 ± 2.03		215.27 ± 0.43		42.18 ± 0.80
0.4		5.497 ± 0.512		172.27 ± 0.19		19.36 ± 0.60		54.95 ± 2.71		213.94 ± 0.47		45.93 ± 0.92
0.6		4.813 ± 0.568		171.85 ± 0.24		18.92 ± 0.74		66.77 ± 3.74		213.96 ± 0.61		48.28 ± 1.19

[a]Main intermolecular/interionic component intraionic vibrational band. [b]$M_1 = (\int \omega I(\omega) d\omega / \int I(\omega) d\omega)$. $I(\omega)$ is the normalized Kerr spectrum by line shape analysis. The integration is made from 0 to 1000 cm^{-1}.

dx.doi.org/10.1021/jp307436t | J. Phys. Chem. B XXXX, XXX, XXX−XXX

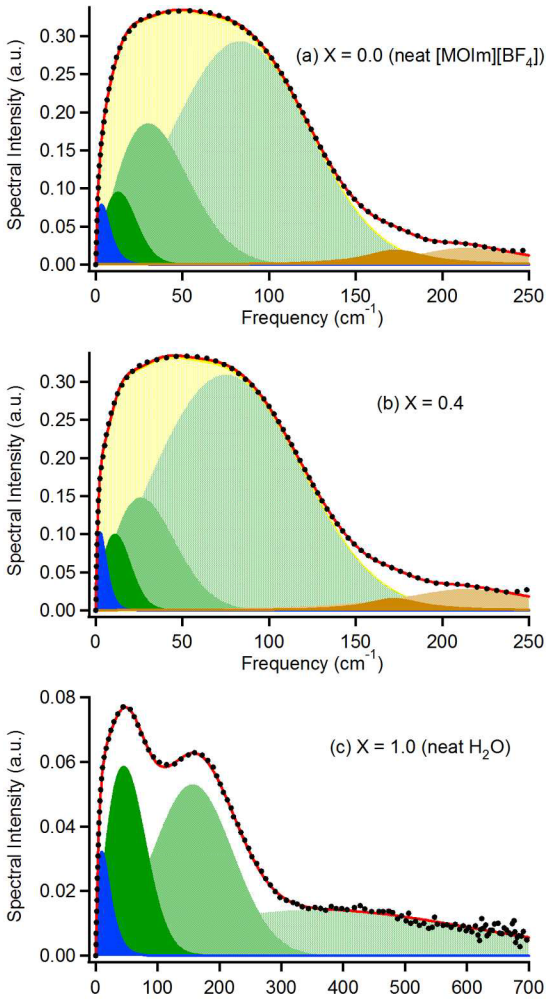

Figure 4. Lineshape analysis results of low-frequency Kerr spectra of (a) neat [OMIm][BF_4] (X = 0.0), (b) [MOIm][BF_4]−H_2O mixture (X = 0.4), and (c) neat H_2O (X = 1.0). Fit ranges are 0−240 cm^{-1} for neat [MOIm][BF_4] and the [MOIm][BF_4]−H_2O mixture (X = 0.4) and 0−700 cm^{-1} for neat H_2O. Black dots denote the Fourier transform Kerr spectra; red solid lines denote the entire fits; blue areas denote the Ohmic functions (eq 1); green areas (dark, medium, and light green) denote the antisymmetrized Gaussian functions (eq 2); brown areas (dark and light brown) denote the Lorentzian functions (eq 3) for the intraionic vibrational modes; and light yellow areas denote the interionic/intermolecular contributions (sum of eqs 1 and 2).

consider here the contribution of "interionic/intermolecular" vibrational band for M_1, and thus the contributions of the "intraionic" vibrational bands and the picosecond overdamped relaxation process, except for the fast relaxation component, are removed. The values of M_1 thus obtained are summarized in Table 3. Even though the value of M_1 for neat H_2O might include some uncertainty for the limitation of the frequency range of the experimentally obtained spectrum, M_1 for neat H_2O estimated in this study is quite similar to that reported in previous work.[84] In the [MOIm][BF_4]−H_2O mixtures, M_1 slightly shifts to the lower frequency with the larger X.

4. DISCUSSION

In the results of the low-frequency Kerr spectra of this study, the most surprising aspect is the X dependence of the low-frequency Kerr spectrum in the [MOIm][BF_4]−H_2O mixtures. As shown in Figure 3(b), the spectral shape is only slightly changed by X. This feature is very different from the fs-RIKES results of IL mixtures with organic solvents such as acetonitrile and CS_2 by Quitevis and co-workers.[32−34] In their results, the line shape of the low-frequency Kerr spectrum in the IL mixtures is very sensitive to the solvent concentration, unlike the present results of the [MOIm][BF_4]−H_2O mixtures. Comparing the present system with the mixtures studied by Quitevis and co-workers, the Kerr signal of H_2O is much weaker than that of [MOIm][BF_4] as shown in Figures 1 and 2, but in contrast, the Kerr signal of acetonitrile and CS_2 is much larger than that of the IL.[32−34] Thus, H_2O does not critically affect the spectral shape in the IL mixtures in comparison with acetonitrile and CS_2.

It is, however, expected that the spectral shape of the low-frequency Kerr spectrum in the [MOIm][BF_4]−H_2O mixtures would be sensitive to X since the low-frequency Kerr spectrum band is a result of the (depolarized Raman active) interionic/intermolecular vibrations. It is rather natural to think that H_2O weakens the interionic interaction between the cation and anion in IL. Our earlier works have demonstrated that the low-frequency Kerr spectrum originates largely from the interionic vibrational motions in the ionic region in the case of aromatic ILs.[18] This is because the spectral shape depends significantly on the anion species, and the librational motions of the imidazolium ring and pyridinium ring appear in this frequency region. Thus, the present results suggest that the microscopic structure and interionic/intermolecular interaction of the ionic region are little influenced by the presence of H_2O within this X range.

We have earlier reported correlations between M_1 of the low-frequency Kerr spectrum band including both the contributions of librations and interaction-induced motions and $(\gamma/d)^{1/2}$ for aprotic molecular liquids[45] and ILs.[18] The idea of the plots is based on the harmonic oscillator. Surely the intermolecular/interionic vibrational band is not identical with the intramolecular/intraionic vibrational mode. Also, the parameters, γ and d, are bulk properties and not directly related to the force constant and reduced mass for the harmonic oscillator. Nonetheless, there is a linear correlation between M_1 of the low-frequency Kerr spectrum and $(\gamma/d)^{1/2}$ for each category of liquids, and thus it is natural to think that that the low-frequency vibrational band is a result of the microscopic interaction that affects the bulk properties. Aromatic ILs have shown a moderate linear correlation,[18] although the slope of the correlation has been found not as steep as for aprotic molecular liquids and nonaromatic ILs. Accordingly, we may think that the near-insensitivity of the interionic/intermolecular vibrational band in the [MOIm][BF_4]−H_2O mixture has been directly transferred to the X dependence of the corresponding d and γ, resulting in near-independences of the latter bulk properties on X for the same mixture.

If we carefully look at the low-frequency spectra of the [MOIm][BF_4]−H_2O mixtures, however, a tiny difference among the spectra for [MOIm][BF_4]−H_2O mixtures, shown in Figure 3, is observed. The spectrum shifts to the lower frequency with the increase of X in the mixture. This result indicates that the interionic interaction of the ionic region of the IL mixture is slightly weakened upon addition of H_2O. Therefore, this result is not inconsistent with the microscopic picture discussed above. Namely, the interfacial H_2O in between the ionic and nonpolar regions slightly weakens the microscopic interionic interaction in the ionic region. Screening

dx.doi.org/10.1021/jp307436t | J. Phys. Chem. B XXXX, XXX, XXX−XXX

by H_2O molecules, as already suggested by simulation studies of mixtures of $[BMIm][BF_4]-H_2O$[85] and 1-hexyl-3-methylimidazolium hexafluorophosphate$-H_2O$,[86] could be responsible for such weakening of the ion−ion interaction in the ILs, but this effect is not extensive in the aspect of the interionic/intermolecular vibrational band.

Localization features of H_2O in imidazolium-based ILs with hydrophilic anions including $[BF_4]^-$ have been explored by several MD simulations.[87−90] In the MD simulation study of $[BMIm][BF_4]-H_2O$ mixtures with X = 0−0.5, Moreno et al. have found that ions are selectively coordinated by individual H_2O molecules in the low X region (<∼0.2), leaving the ionic network largely unperturbed.[87] In the high X region, however, the ionic network is disrupted/swollen by H_2O clusters (X = 0.5). It can be expected that the presence of H_2O near the ionic region and the swollen structure of the ionic network are a result of softening the interionic interaction (and thus a red shift of the vibrational band) in the ionic region. This picture is therefore in overall agreement with the present results of the low-frequency Kerr spectrum. The present data shown in Figure 3(b) and Table 3 show almost overlapping spectra are obtained in the X range of 0−0.4, but a slight red shift can be seen at X = 0.6 in the mixture.

On the basis of FT-IR studies, it is well-known that H_2O in imidazolium cation based ILs with $[BF_4]^-$ interacts dominantly with the anion rather than the cation.[21,24] Previously, we have investigated the $[MOIm][BF_4]-H_2O$ mixtures by means of conventional FT-IR and Raman spectroscopies and a solvatochromic probe (betaine 33).[30] The symmetric F−B stretching mode of the $[BF_4]^-$ anion shifts to the higher frequency side with the larger X. In fact, other intraionic vibrational modes of the imidazolium ring also shift to the higher frequency with the addition of H_2O.[22,27] The shift of the intraionic vibrational modes by addition of H_2O is opposite to that of the interionic/intermolecular vibrational band. However, this is not surprising. In the case of intraionic vibrational modes, the weakened interionic/intermolecular interaction by H_2O induces stronger bond strength of the ions. On the other hand, the interionic/intermolecular vibrational band is directly related to the interionic/intermolecular interaction. Thus, the direction of the shift of the vibrational frequency of the interionic vibrational band with X is opposite to that found for the intraionic vibrational band. In the present study, we have also observed that the intraionic vibrational modes at ca. 172 and 214 cm^{-1} show almost no modification with the increase of the water mole fraction X in the binary mixture. Since the vibrational modes are due to the octyl group of the cation, which composes the nonpolar region in the IL/H_2O mixture, they are least influenced by the addition of H_2O.

Takamuku et al. have recently investigated 1-ethyl-3-methylimidazolium tetrafluoroborate ($[EMIm][BF_4]$) and H_2O mixtures using several techniques including FT-IR, NMR, and large-angle X-ray diffraction.[27] Their FT-IR measurements have revealed that the peaks of the vibrational modes of the three H−Cs of the imidazolium ring undergo a small change upon addition of H_2O. The X-ray results, on the other hand, show that the distance between the $[BF_4]^-$ anion and the 2 position carbon C(2), which is in between the nitrogen atoms of the imidazolium ring, becomes closer from X = 0.10 to X = 0.33, but that between the $[BF_4]^-$ anion and the 4 and 5 position carbons does not change. They have interpreted that this is evidence for the early stage of formation of the ion pair upon addition of H_2O in $[EMIm][BF_4]$. The overall picture that these results depict is that the specific interaction between the H−C(2) of the imidazolium ring and the anion becomes stronger and, as a result, is somewhat inconsistent with the present study. This inconsistency may have originated from the difference in the length scale probed by the fs-RIKES experiments and involved in the X-ray results. Namely, the RIKES dominantly probes the ionic region which is longer length scale than the length scale involved in the X-ray diffraction results by Takamuku and co-workers.[27] The X-ray results focus on the specific ion pair in the IL/H_2O mixture, but the Kerr spectrum obtained by RIKES includes many-body interactions of cations and anions, as well as of ions and water. Accordingly, these results obtained by different techniques suggest that the "specific" interionic interaction of a cation and anion pair in the IL/H_2O mixture becomes stronger with addition of H_2O, but the "many-body" interionic interaction of the ionic region in the binary mixture becomes weaker.

In contrast to the low-frequency vibrational spectra, the picosecond overdamped relaxation process depends strongly on X, as shown in Figure 1b and Table 2. The average relaxation time $<\tau>$ increases with increasing X. This feature is counterintuitive because the shear viscosity of IL decreases upon addition of H_2O (see Table 1). Recently, Fayer and co-workers have investigated the overdamped picosecond relaxation process of IL mixtures with H_2O by femtosecond RIKES.[38] According to their study, the slowest relaxation time constant (which is attributed to α-relaxation process) of neat $[MOIm][BF_4]$ is about 10 ns and decreases with X (down to 5.7 ns for the mixture at X = 0.5). At a first glance, therefore, the present results (Table 2) appear to be inconsistent with those of Fayer and co-workers and the Stokes−Einstein−Debye hydrodynamic model predictions.[91,92] Since the actual slowest relaxation time is in the nanosecond time scale,[38] the present fs-RIKES measurements can capture only a part of this slow relaxation or more likely the process prior to the actual slowest relaxation process. Although the value of the offset parameter a_0 is not directly correlated to the actual slowest relaxation time, this is evidence of the presence of a slower relaxation process or processes: the magnitude of the Kerr intensity must be null if the slowest relaxation process is completed within the present time window.

The time constants (and average time constant) obtained by the fits to the overdamped relaxation process becoming slower with the increasing X in the IL mixture cannot be explained by the simple Stokes−Einstein−Debye hydrodynamic model.[91,92] One possibility is that this relaxation process is influenced by the interionic/intermolecular vibrations. In contrast to the orientational relaxation in solution, the low-frequency Kerr spectrum arising from the interionic/intermolecular vibrational dynamics shifts to a higher frequency (and thus associates with a faster time scale) as intermolecular interaction strengthens. Recent MD simulation by Margulis and co-workers[93] showed that the interaction-induced motion in the interionic vibrational dynamics in an IL is very slow compared to the interaction-induced motion of simple molecular liquids. This indicates that the retarded interionic vibrational dynamics in the IL (and the IL mixtures) is likely to appear at the time scale of picoseconds or even slower like an overdamped relaxation process, and this relaxation is more elastic in nature than hydrodynamic. Therefore, it is plausible that the time constant of this time scale relaxation in the IL/H_2O mixture (and also neat IL) is not simply correlated to the shear viscosity.

dx.doi.org/10.1021/jp307436t | J. Phys. Chem. B XXXX, XXX, XXX−XXX

5. SUMMARY

We have investigated the interionic/intermolecular dynamics of mixtures of [MOIm][BF_4] with H_2O by means of fs-RIKES. Addition of H_2O in this IL produces a small red shift in the low-frequency Kerr spectrum of [MOIm][BF_4]−H_2O mixtures. In the IL/H_2O mixtures, the major contribution to the RIKES spectrum comes from the aromatic moiety of the cation. The tiny red shift in the low-frequency Kerr spectrum upon addition of H_2O is attributed to the slight weakening of the interionic/intermolecular interaction in the ionic region, not the nonpolar region. On the other hand, the picosecond overdamped relaxation process is very sensitive to X. The picosecond overdamped relaxation process in the [MOIm][BF_4]−H_2O mixtures has been fitted to a triexponential function with an offset component. With addition of H_2O, all the three relaxation time constants become larger, but the offset component becomes smaller. Taking the results of the α-relaxation process of IL−H_2O mixtures by Fayer and co-workers[38] into consideration, the observed feature of the picosecond overdamped relaxation process in this study implies that the offset component can be largely attributed to the slowest relaxation process (α-relaxation), and this relaxation process becomes faster with the increasing X since the shear viscosity decreases with the increasing X in the IL mixture.

AUTHOR INFORMATION

Corresponding Author

*E-mail: shirota@faculty.chiba-u.jp; ranjit@bose.res.in.

Notes

The authors declare no competing financial interest.

ACKNOWLEDGMENTS

We would like to thank Prof. Ralf Ludwig (University of Rostock) for helpful discussion. RB's stay at Chiba was supported by Center for Frontier Science, Chiba University. This study was supported by the Ministry of Education, Culture, Sports, Science and Technology (MEXT) of Japan (Grant-in-Aid for Young Scientists (A), 21685001: HS). RB would like to thank the Director of S. N. Bose National Centre for Basic Sciences for encouragement.

REFERENCES

(1) Wang, Y.; Voth, G. A. *J. Am. Chem. Soc.* **2005**, *127*, 12192−12193.
(2) Wang, Y.; Voth, G. A. *J. Phys. Chem. B* **2006**, *110*, 18601−18608.
(3) Lopes, J. N. A. C.; Padua, A. A. H. *J. Phys. Chem. B* **2006**, *110*, 3330−3335.
(4) Lopes, J. N. C.; Gomes, M. F. C.; Padua, A. A. H. *J. Phys. Chem. B* **2006**, *110*, 16816−16818.
(5) Samanta, A. *J. Phys. Chem. B* **2006**, *110*, 13704−13716.
(6) Hu, Z. H.; Margulis, C. J. *Proc. Natl. Acad. Sci. U.S.A.* **2006**, *103*, 831−836.
(7) Iwata, K.; Okajima, H.; Saha, S.; Hamaguchi, H.-O. *Acc. Chem. Res.* **2007**, *40*, 1174−1181.
(8) Triolo, A.; Russina, O.; Bleif, H.-J.; Di Cola, E. *J. Phys. Chem. B* **2007**, *111*, 4641−4644.
(9) Mizuhata, M.; Maekawa, M.; Deki, S. *ECS Trans.* **2007**, *3*, 89−95.
(10) Xiao, D.; Rajian, J. R.; Cady, A.; Li, S.; Bartsch, R. A.; Quitevis, E. L. *J. Phys. Chem. B* **2007**, *111*, 4669−4677.
(11) Atkin, R.; Warr, G. G. *J. Phys. Chem. B* **2008**, *112*, 4164−4166.
(12) Triolo, A.; Russina, O.; Fazio, B.; Appetecchi, G. B.; Carewska, M.; Passerini, S. *J. Chem. Phys.* **2009**, *130*, 164521/1−6.
(13) Russina, O.; Triolo, A.; Gontrani, L.; Caminiti, R.; Xiao, D.; Hines, L. G., Jr.; Bartsch, R. A.; Quitevis, E. L.; Plechkova, N.; Seddon, K. R. *J. Phys.: Condens. Matter* **2009**, *21*, 424121/1−9.
(14) Zheng, W.; Mohammed, A.; Larry, G.; Hines, J.; Xiao, D.; Martinez, O. J.; Bartsch, R. A.; Simon, S. L.; Russina, O.; Triolo, A.; Quitevis, E. L. *J. Phys. Chem. B* **2011**, *115*, 6572−6584.
(15) Castner, E. W., Jr.; Margulis, C. J.; Maroncelli, M.; Wishart, J. F. *Annu. Rev. Phys. Chem.* **2011**, *62*, 85−105.
(16) Triolo, A.; Russina, O.; Caminiti, R.; Shirota, H.; Lee, H. Y.; Santos, C. S.; Murthy, N. S.; Edward W. Castner, J. *Chem. Commun.* **2012**, *48*, 4959−4961.
(17) Sahu, K.; Kern, S. J.; Berg, M. A. *J. Phys. Chem. A* **2011**, *115*, 7984−7993.
(18) Shirota, H. *ChemPhysChem* **2012**, *13*, 1638−1648.
(19) *Ionic Liquids in Synthesis*, 2 ed.; Wasserscheid, P., Welton, T., Eds.; Wiley-VCH: Weinheim, 2008.
(20) *Ionic Liquids: Theory, Properties, New Approaches*; Kokorin, A., Ed.; InTech: Rijeka, 2011.
(21) Cammarata, L.; Kazarian, S. G.; Salter, P. A.; Welton, T. *Phys. Chem. Chem. Phys.* **2001**, *3*, 5192−5200.
(22) Jeon, Y.; Sung, J.; Kim, D.; Seo, C.; Cheong, H.; Ouchi, Y.; Ozawa, R.; Hamaguchi, H.-o. *J. Phys. Chem. B* **2008**, *112*, 923−928.
(23) Jeon, Y.; Sung, J.; Seo, C.; Lim, H.; Cheong, H.; Kang, M.; Moon, B.; Ouchi, Y.; Kim, D. *J. Phys. Chem. B* **2008**, *112*, 4735−4740.
(24) Danten, Y.; Cabao, M. I.; Besnard, M. *J. Phys. Chem. A* **2009**, *113*, 2873−2889.
(25) Umebayashi, Y.; Jiang, J.-C.; Shan, Y.-L.; Lin, K.-H.; Fujii, K.; Seki, S.; Ishiguro, S.-I.; Lin, S. H.; Chang, H.-C. *J. Chem. Phys.* **2009**, *130*, 124503/1−6.
(26) Koddermann, T.; Wertz, Christiane; Heintz, A.; Ludwig, R. *Angew. Chem., Int. Ed. Engl.* **2006**, *45*, 3697−3702.
(27) Takamuku, T.; Kyoshoin, Y.; Shimomura, T.; Kittaka, S.; Yamaguchi, T. *J. Phys. Chem. B* **2009**, *113*, 10817−10824.
(28) Shimomura, T.; Fujii, K.; Takamuku, T. *Phys. Chem. Chem. Phys.* **2010**, *12*, 12316−12324.
(29) Shimomura, T.; Takamuku, T.; Yamaguchi, T. *J. Phys. Chem. B* **2011**, *115*, 8515−8527.
(30) Masaki, T.; Nishikawa, K.; Shirota, H. *J. Phys. Chem. B* **2010**, *114*, 6323−6331.
(31) Roth, C.; Appelhagen, A.; Jobst, N.; Ludwig, R. *ChemPhysChem* **2012**, *13*, 1708−1717.
(32) Xiao, D.; Hines, L. G., Jr.; Bartsch, R. A.; Quitevis, E. L. *J. Phys. Chem. B* **2009**, *113*, 4544−4548.
(33) Yang, P.; Voth, G. A.; Xiao, D.; Hines, L. G., Jr.; Bartsch, R. A.; Quitevis, E. L. *J. Chem. Phys.* **2011**, *135*, 034502/1−12.
(34) Bardak, F.; Xiao, D.; Hines, L. G., Jr.; Son, P.; Bartsch, R. A.; Quitevis, E. L.; Yang, P.; Voth, G. A. *ChemPhysChem* **2012**, *13*, 1687−1700.
(35) Koeberga, M.; Wu, C.-C.; Kimc, D.; Bonn, M. *Chem. Phys. Lett.* **2007**, *439*, 60−64.
(36) Sando, G. M.; Dahl, K.; Owrutsky, J. C. *J. Phys. Chem. B* **2007**, *111*, 4901−4909.
(37) Kashyap, H. K.; Biswas, R. *J. Phys. Chem. B* **2010**, *114*, 254−268.
(38) Sturlaugson, A. L.; Fruchey, K. S.; Fayer, M. D. *J. Phys. Chem. B* **2012**, *116*, 1777−1787.
(39) Anthony, J. L.; Maginn, E. J.; Brennecke, J. F. *J. Phys. Chem. B* **2001**, *105*, 10942−10949.
(40) Lotshaw, W. T.; McMorrow, D.; Thantu, N.; Melinger, J. S.; Kitchenham, R. *J. Raman Spectrosc.* **1995**, *26*, 571−583.
(41) Kinoshita, S.; Kai, Y.; Ariyoshi, T.; Shimada, Y. *Int. J. Mod. Phys. B* **1996**, *10*, 1229−1272.
(42) Castner, E. W., Jr.; Maroncelli, M. *J. Mol. Liq.* **1998**, *77*, 1−36.
(43) Smith, N. A.; Meech, S. R. *Int. Rev. Phys. Chem.* **2002**, *21*, 75−100.
(44) Zhong, Q.; Fourkas, J. T. *J. Phys. Chem. B* **2008**, *112*, 15529−15539.
(45) Shirota, H.; Fujisawa, T.; Fukazawa, H.; Nishikawa, K. *Bull. Chem. Soc. Jpn.* **2009**, *82*, 1347−1366.

(46) Loughnane, B. J.; Farrer, R. A.; Scodinu, A.; Reilly, T.; Fourkas, J. T. *J. Phys. Chem. B* **2000**, *104*, 5421−5429.
(47) Farrer, R. A.; Fourkas, J. T. *Acc. Chem. Res.* **2003**, *36*, 605−612.
(48) Hunt, N. T.; Jaye, A. A.; Meech, S. R. *Phys. Chem. Chem. Phys.* **2007**, *9*, 2167−2180.
(49) Castner, E. W., Jr.; Wishart, J. F.; Shirota, H. *Acc. Chem. Res.* **2007**, *40*, 1217−1227.
(50) Shirota, H.; Fukazawa, H. Atom Substitution Effects in Ionic Liquids: A Microscopic View by Femtosecond Raman-Induced Kerr Effect Spectroscopy. In *Ionic Liquids: Theory, Properties, New Approaches*; Kokorin, A., Ed.; InTech: Rijeka, Croatia, 2011; pp 201−224.
(51) Khalil, M.; Golonzka, O.; Demirdoven, N.; Fecko, C. J.; Tokmakoff, A. *Chem. Phys. Lett.* **2000**, *321*, 231−237.
(52) Wiewior, P. P.; Shirota, H.; Castner, E. W., Jr. *J. Chem. Phys.* **2002**, *116*, 4643−4654.
(53) Heisler, I. A.; Meech, S. R. *J. Chem. Phys.* **2010**, *132*, 174503/1−7.
(54) Shirota, H. *J. Chem. Phys.* **2005**, *122*, 044514/1−12.
(55) Shirota, H. *J. Phys. Chem. A* **2011**, *115*, 14262−14275.
(56) Seddon, K. R.; Stark, A.; Torres, M. J. *ACS Symp. Ser.* **2002**, *819*, 34−49.
(57) Sanchez, L. G.; Espel, J. R.; Onink, F.; Meindersma, G. W.; Haan, A. B. d. *J. Chem. Eng. Data* **2009**, *54*, 2803−2812.
(58) Restolho, J.; Serro, A. P.; Mata, J. L.; Saramago, B. *J. Chem. Eng. Data* **2009**, *54*, 950−955.
(59) *CRC Handbook of Chemistry and Physics*, 89th ed.; Lide, D. R., Ed.; CRC Press: Boca Raton, 2008.
(60) Liu, W.; Cheng, L.; Zhang, Y.; Wang, H.; Yu, M. *J. Mol. Liq.* **2008**, *140*, 68−72.
(61) Ries, L. A. S.; Amaral, F. A. d.; Matos, K.; Martini, E. M. A.; de Souza, M. O.; de Souza, R. F. *Polyhedron* **2008**, *27*, 3287−3293.
(62) Rilo, E.; Pico, J.; Garcia-Garabal, S.; Varela, L. M.; Cabeza, O. *Fluid Phase Equilib.* **2009**, *285*, 83−89.
(63) McMorrow, D.; Lotshaw, W. T. *Chem. Phys. Lett.* **1990**, *174*, 85−94.
(64) McMorrow, D.; Lotshaw, W. T. *J. Phys. Chem.* **1991**, *95*, 10395−10406.
(65) Loughnane, B. J.; Scodinu, A.; Farrer, R. A.; Fourkas, J. T.; Mohanty, U. *J. Chem. Phys.* **1999**, *111*, 2686−2694.
(66) Loughnane, B. J.; Scodinu, A.; Fourkas, J. T. *J. Phys. Chem. B* **2006**, *110*, 5708−5720.
(67) McMorrow, D.; Thantu, N.; Kleiman, V.; Melinger, J. S.; Lotshaw, W. T. *J. Phys. Chem. A* **2001**, *105*, 7960−7972.
(68) Shirota, H.; Castner, E. W., Jr. *J. Phys. Chem. A* **2005**, *109*, 9388−9392.
(69) Shirota, H.; Castner, E. W., Jr. *J. Phys. Chem. B* **2005**, *109*, 21576−21585.
(70) Shirota, H.; Wishart, J. F.; Castner, E. W., Jr. *J. Phys. Chem. B* **2007**, *111*, 4819−4829.
(71) Shirota, H.; Nishikawa, K.; Ishida, T. *J. Phys. Chem. B* **2009**, *113*, 9831−9839.
(72) Fujisawa, T.; Nishikawa, K.; Shirota, H. *J. Chem. Phys.* **2009**, *131*, 244519/1−14.
(73) Shirota, H.; Fukazawa, H.; Fujisawa, T.; Wishart, J. F. *J. Phys. Chem. B* **2010**, *114*, 9400−9412.
(74) Fukazawa, H.; Ishida, T.; Shirota, H. *J. Phys. Chem. B* **2011**, *115*, 4621−4631.
(75) Shirota, H.; Ishida, T. *J. Phys. Chem. B* **2011**, *115*, 10860−10870.
(76) Bucaro, J. A.; Litovitz, T. A. *J. Chem. Phys.* **1971**, *54*, 3846−3853.
(77) Chang, Y. J.; Castner, E. W., Jr. *J. Chem. Phys.* **1993**, *99*, 7289−7299.
(78) Hyun, B. R.; Dzyuba, S. V.; Bartsch, R. A.; Quitevis, E. L. *J. Phys. Chem. A* **2002**, *106*, 7579−7585.
(79) Rajian, J. R.; Li, S. F.; Bartsch, R. A.; Quitevis, E. L. *Chem. Phys. Lett.* **2004**, *393*, 372−377.
(80) Xiao, D.; Rajian, J. R.; Li, S. F.; Bartsch, R. A.; Quitevis, E. L. *J. Phys. Chem. B* **2006**, *110*, 16174−16178.
(81) Xiao, D.; Rajian, J. R.; Hines, L. G., Jr.; Li, S.; Bartsch, R. A.; Quitevis, E. L. *J. Phys. Chem. B* **2008**, *112*, 13316−13325.
(82) Xiao, D.; Hines, L. G., Jr.; Li, S.; Bartsch, R. A.; Quitevis, E. L.; Russina, O.; Triolo, A. *J. Phys. Chem. B* **2009**, *113*, 6426−6433.
(83) Xiao, D.; Hines, L. G., Jr.; Holtz, M. W.; Song, K.; Bartsch, R. A.; Quitevis, E. L. *Chem. Phys. Lett.* **2010**, *497*, 37−42.
(84) Shirota, H.; Ushiyama, H. *J. Phys. Chem. B* **2008**, *112*, 13542−13551.
(85) Schroder, C.; Rudas, T.; Neumayr, G.; Benkner, S.; Steinhauser, O. *J. Chem. Phys.* **2007**, *127*, 234503−234501.
(86) Annapureddy, H. V. R.; Hu, Z.; Xia, J.; Margulis, C. J. *J. Phys. Chem. B* **2008**, *112*, 1770−1776.
(87) Moreno, M.; Castiglione, F.; Mele, A.; Pasqui, C.; Raos, G. *J. Phys. Chem. B* **2008**, *112*, 7826−7836.
(88) Porter, A. R.; Liem, S. Y.; Popelier, P. L. A. *Phys. Chem. Chem. Phys.* **2008**, *10*, 4240−4248.
(89) Bhargava, B. L.; Klein, M. L. *J. Phys. Chem. A* **2009**, *113*, 1898−1904.
(90) Feng, S.; Voth, G. A. *Fluid Phase Equilib.* **2010**, *294*, 148−156.
(91) Dote, J. L.; Kivelson, D.; Schwartz, R. N. *J. Phys. Chem.* **1981**, *85*, 2169−2180.
(92) Fleming, G. R. *Chemical Applications of Ultrafast Spectroscopy*; Oxford University Press: New York, 1986.
(93) Hu, Z.; Huang, X.; Annapureddy, H. V. R.; Margulis, C. J. *J. Phys. Chem. B* **2008**, *112*, 7837−7849.